Fe(II)-Catalyzed Recrystallization of Goethite Revisited

ARTICLE *in* ENVIRONMENTAL SCIENCE AND TECHNOLOGY · SEPTEMBER 2014

Impact Factor: 5.33 · DOI: 10.1021/es503084u · Source: PubMed

11 AUTHORS, INCLUDING:

Robert Handler
Michigan Technological University
33 PUBLICATIONS **369** CITATIONS
SEE PROFILE

Andrew J Frierdich
Monash University (Australia)
15 PUBLICATIONS **192** CITATIONS
SEE PROFILE

Kevin M. Rosso
Pacific Northwest National Laboratory
181 PUBLICATIONS **4,728** CITATIONS
SEE PROFILE

Drew Latta
University of Iowa
15 PUBLICATIONS **237** CITATIONS
SEE PROFILE

Environmental Science & Technology

Article

pubs.acs.org/est

Fe(II)-Catalyzed Recrystallization of Goethite Revisited

Robert M. Handler,[†,#] Andrew J. Frierdich,[‡,§,#] Clark M. Johnson,[§] Kevin M. Rosso,[∥] Brian L. Beard,[§] Chongmin Wang,[∥] Drew E. Latta,[‡] Anke Neumann,[‡,⊥] Timothy Pasakarnis,[‡] W. A. P. J. Premaratne,[‡] and Michelle M. Scherer*[,‡]

[†]Sustainable Futures Institute, Michigan Technological University 1400 Townsend Drive, Houghton, Michigan 49931, United States

[‡]Department of Civil and Environmental Engineering, University of Iowa, Iowa City, Iowa 52242, United States

[§]Department of Geoscience, University of Wisconsin, Madison, Wisconsin 53706, United States

[∥]Pacific Northwest National Laboratory, Richland, Washington 99352, United States

Supporting Information

ABSTRACT: Results from enriched ^{57}Fe isotope tracer experiments have shown that atom exchange can occur between structural Fe in Fe(III) oxides and aqueous Fe(II) with no formation of secondary minerals or change in particle size or shape. Here we derive a mass balance model to quantify the extent of Fe atom exchange between goethite and aqueous Fe(II) that accounts for different Fe pool sizes. We use this model to reinterpret our previous work and to quantify the influence of particle size and pH on extent of goethite exchange with aqueous Fe(II). Consistent with our previous interpretation, substantial exchange of goethite occurred at pH 7.5 (≈ 90%) and we observed little effect of particle size between nanogoethite (average size of 81 × 11 nm; ≈ 110 m^2/g) and microgoethite (average size of 590 × 42 nm; ≈ 40 m^2/g). Despite ≈90% of the bulk goethite exchanging at pH 7.5, we found no change in mineral phase, average particle size, crystallinity, or reactivity after reaction with aqueous Fe(II). At a lower pH of 5.0, no net sorption of Fe(II) was observed and significantly less exchange occurred accounting for less than the estimated proportion of surface Fe atoms in the particles. Particle size appears to influence the amount of exchange at pH 5.0 and we suggest that aggregation and surface area may play a role. Results from sequential chemical extractions indicate that ^{57}Fe accumulates in extracted Fe(III) goethite components. Isotopic compositions of the extracts indicate that a gradient of ^{57}Fe develops within the goethite with more accumulation of ^{57}Fe occurring in the more easily extracted Fe(III) that may be nearer to the surface.

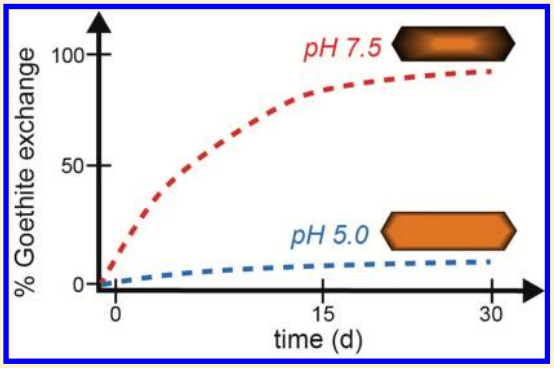

INTRODUCTION

Iron is the most abundant redox-active metal on Earth, and commonly occurs in sedimentary environments as Fe(III) (hydr)oxide minerals. Under reducing conditions at the Earth's near surface, fluxes of aqueous Fe(II) at Fe(III) mineral surfaces may be generated by microbial dissimilatory iron reduction (DIR) coupled to oxidation of organic carbon[1−3] as well as chemical and physical weathering of Fe bearing minerals.[4] Ferrous Fe generated from microbial respiration and weathering of Fe bearing minerals has been shown to influence the dissolution, secondary mineral precipitation, and bioreducibility of Fe(III) oxides[5−9] and has been linked to critical environmental processes including contaminant and trace element dynamics in groundwater, sediments, and modern seawater.[10−25] The term Fe(III) oxides will be used to refer to both Fe(III) oxides and oxyhydroxides.

Reaction of aqueous Fe(II) with some of the more unstable Fe oxides is well-known to result in recrystallization and formation of new product minerals (e.g., the transformation of ferrihydrite to goethite, or lepidocrocite to magnetite).[6,9,26,27] For more stable Fe oxides, such as goethite and magnetite, however, reaction with aqueous Fe(II) does not induce any obvious new mineral products, and until recently, the reaction of aqueous Fe(II) with these more stable Fe(III) oxides was viewed as a sorption−desorption reaction at the oxide surface with no consideration of recrystallization of the bulk oxide. Compelling evidence from Fe isotope studies, however, shows that exchange of Fe atoms between the aqueous phase and bulk oxide occurs even in some of these more stable Fe oxides, leading us and others to suggest that Fe(II)-catalyzed mineral recrystallization is taking place.[9,28−33]

The extent to which Fe oxides can exchange atoms with aqueous Fe(II) is known for only a few pure minerals,[28,33] and it has been shown that surface adsorption of Si and organic matter,[34,35] and isomorphic Al-substitution[36−38] can inhibit Fe atom exchange. In addition, recent work has shown that Fe(II)-catalyzed recrystallization can lead to release and incorporation

Received: June 25, 2014
Revised: September 7, 2014
Accepted: September 8, 2014
Published: September 23, 2014

of other metals such as Ni, Zn, Cu, Co, and Mn.[39−42] In a study of Fe(II) interaction with hematite single crystals, a bulk conduction mechanism was proposed that provides an explanation for exchange of Fe atoms with Fe(III) oxides based on Fe(II) sorption to the mineral surface, electron transfer from sorbed Fe(II) to Fe(III) in the underlying mineral, bulk electron conduction, and reductive dissolution of structural Fe(III) at another crystallographic site, thereby regenerating $Fe(II)_{aq}$.[43] We have proposed that this mechanism may explain observations of Fe(II)-catalyzed recrystallization of goethite.[9,28,32] For recent reviews of these studies and the emergence of a revised conceptual model for Fe(II) sorption on Fe oxides, see refs 42 and 44.

Two approaches have been used to quantify the extent to which Fe oxides can exchange with aqueous Fe(II). The first approach is based on mass balance modeling of natural, mass-dependent isotope fractionation to estimate Fe atom exchange,[29,30,32,45,46] whereas the second approach employs enriched isotope tracers (e.g., ^{55}Fe and ^{57}Fe) to directly track Fe atom exchange.[9,28,33−37,47] Significant disparity exists among amounts of exchange reported even for a single oxide. Reported extents of exchange for goethite, for example, with aqueous Fe(II) vary between ∼4 and 100%.[9,28,37,47] Reconciling the differences between these studies is difficult since different reaction conditions (e.g., pH and Fe(II):Fe(III) ratio) and different approaches to estimate the extent of Fe atom exchange were used. The majority of studies using natural, mass-dependent isotope fractionation report that approximately one monolayer of the mineral surface was open to atom exchange with aqueous Fe(II). The extent of exchange in these experiments, however, was not directly measured but rather calculated based on extrapolations of small compositional changes (∼1‰) to operationally defined reactive Fe components.

Here, we explore the effect of pH and particle size on the extent of exchange between aqueous Fe(II) and goethite using a ^{57}Fe-enriched isotope tracer approach similar to our previous work. Importantly, we derive a mass balance model to quantify the extent of Fe atom exchange between Fe pools (e.g., $Fe(II)_{aq}$ and goethite) that accounts for different Fe pool sizes, and we use this model to recalculate the extent of exchange estimated in our previous work and to quantify the influence of particle size and pH on the extent of goethite exchange with aqueous Fe(II). We highlight the distinction between percent of solid Fe atoms exchanged and fractional approach to complete mixing of the enriched isotope tracer. We also use sequential chemical extractions to measure the isotopic composition of different Fe components and characterize the goethite particles before and after reaction with Fe(II).

MATERIALS AND METHODS

Materials. All chemicals were ACS reagent grade or better and used as received, except for HCl which was further purified through sub-boiling distillation. Deionized water (>18 MΩ cm) was used to make all solutions, and was made anoxic by sparging with N_2 gas. Ferric nitrate ($Fe(NO_3)_3{\cdot}9H_20$), sodium bicarbonate ($NaHCO_3$), and potassium hydroxide (KOH) were used in goethite synthesis. Experimental buffer solutions were made from either 4-(2-hydroxyethyl)-1-piperazineethanesulfonic acid (HEPES) and potassium bromide (KBr) or acetic acid. Aqueous Fe(II) stocks were prepared by dissolving ^{57}Fe metal (Chemgas, 96% ^{57}Fe) and natural abundance anhydrous ferrous chloride ($FeCl_2$) in 0.5 M HCl. Chemical reductive dissolution experiments were performed using L-ascorbic acid.

Goethite Synthesis and Characterization. Synthesis procedures for goethite particles used in this study have been described previously.[48] Briefly, the method of Burleson and Penn[49] was modified for preparation of goethite nanorods. $NaHCO_3$ (0.48 M, 500 mL) was added to 500 mL of 0.4 M $Fe(NO_3)_3{\cdot}9H_2O$ in a dropwise fashion to generate a ferrihydrite intermediate, which was microwaved to boiling and quickly cooled in an ice bath. After dialysis, the suspension pH was raised to 13 with 5 M NaOH and heated at 90 °C for 24 h to generate nanogoethite. Microgoethite particles were synthesized using the method of Schwertmann and Cornell, through quick addition of KOH to $Fe(NO_3)_3{\cdot}9H_2O$ and heating for 60 h at 70 °C.[50] These samples of goethite have been characterized and used in previous studies.[28,48] X-ray diffraction (XRD) patterns of each sample did not display any peaks indicative of other Fe minerals. Specific surface areas as determined by N_2−BET measurements were 40 ± 3 m^2/g and 110 ± 7 m^2/g for microgoethite and nanogoethite, respectively.

After reaction with aqueous Fe(II) for 30 days, selected reactors were sacrificed for solids characterization. Reactor contents were passed through a syringe filter housing equipped with a 0.45 μm removable filter disc, and solids were removed and rinsed with deionized water. For XRD analysis, solids were combined with a small amount of glycerol and the slurry was placed on a specimen holder and analyzed using a Rigaku Miniflex II equipped with a Co X-ray source. Separate samples were prepared for transmission electron microscopy (TEM) by placing rinsed solids on a carbon-coated Cu grid. Images were collected using a JEOL JEM 1230 microscope and analysis of resulting images was performed with ImageJ software (http://rsbweb.nih.gov/ij/). Goethite samples intended for high-resolution electron microscopy (HR-TEM) were resuspended in ethanol to reduce particle aggregation and a fraction of these samples were deposited on a holey carbon grid. Another fraction was dried anoxically. HR-TEM was performed at the Environmental Molecular Sciences Laboratory in Richland, WA, on a JEOL JEM-2010 TEM with a LaB_6 filament and post column attached with a Gatan Image Filter (GIF2000). The acceleration voltage on the microscope was 200 kV. Images were collected of both the grid-deposited powders, and of thin sections of dried powder suspended in epoxy resin.

Enriched Fe Isotope Tracer Experiments. All experiments were carried out in an anoxic glovebox equipped with multiple Pd-catalysts for oxygen scrubbing, and great care was taken to prevent O_2 intrusion into the reactors during centrifugation. Fe(II) isotope tracer experiments were initiated using procedures described previously.[28] Briefly, 15 mL of a pH 7.5 HEPES (25 mM) or pH 5.0 acetic acid buffer solution (5 mM) was spiked to ∼1 mM Fe(II) with an Fe(II) stock that had been enriched in ^{57}Fe ($\delta^{57/56}Fe$ = +840.43‰). After equilibrating for 1 h, batch reactors were filtered with a 0.2 μm filter into a 30 mL Nalgene centrifuge tube and the initial Fe(II) concentration was measured. Goethite particles were added (30 mg, 2 g/L solids loading), and batch reactors were placed on an end-overend rotator to mix in the dark for times ranging from 10 min to 30 days. To sample ^{57}Fe(II) tracer experiments, reactors were sacrificed for separation into five operationally defined components (aqueous Fe(II), *extract* 1, *extract* 2, *extract* 3, and goethite solids) using a series of successive acid extractions described in detail in the Supporting Information (SI) (Table S1). Subsamples of aqueous solution

and sequential extractions were analyzed for Fe(II) and Fe(III). Aqueous Fe(II) concentrations were determined using the phenanthroline method.[51] Fluoride was added to remove potential interferences from aqueous Fe(III).[52] Fe(III) concentrations were determined by difference between aqueous Fe(II) samples and separate subsamples in which all aqueous Fe was reduced to Fe(II) with hydroxylamine HCl.[51]

Fe Isotope Measurements. Prior to chemical separation, all Fe samples were oxidized by evaporating the sample to dryness with HNO_3. Samples were purified using anion exchange chromatography and Fe isotopes were analyzed using a Micromass *IsoProbe* single focusing MC-ICP-MS according to previously established methods that are proven to be free of sample matrix effects.[28,53,54] Isotopic compositions are expressed in delta notation:

$$\delta^{57/56}\mathrm{Fe}(‰) = \left(\frac{\frac{^{57}\mathrm{Fe}}{^{56}\mathrm{Fe}_{\mathrm{sample}}} - \frac{^{57}\mathrm{Fe}}{^{56}\mathrm{Fe}_{\mathrm{std}}}}{\frac{^{57}\mathrm{Fe}}{^{56}\mathrm{Fe}_{\mathrm{std}}}} \right) \times 1000 \quad (1)$$

where $(^{57}\mathrm{Fe}/^{56}\mathrm{Fe})_{\mathrm{std}}$ is the average isotopic ratio for terrestrial igneous rocks.[55] Based on replicate analyses of 33 samples passed through the entire analytical process, the average 1-standard deviation uncertainty in measured $\delta^{57/56}$Fe values is 0.13‰.[52]

Reductive Dissolution Experiments. Procedures for reductive dissolution experiments were adapted from Postma.[56] Goethite solids were mixed for 30 days in the presence or absence of 1 mM Fe(II) in accordance with the experimental protocol for isotope exchange experiments. Solids were then collected and rinsed with deionized water to remove residual aqueous Fe(II) through centrifugation and resuspension in HEPES buffer solution. To initiate dissolution experiments at pH 3, 10 mg of goethite solids were resuspended in 120 mL of 10 mM ascorbic acid (solids loading ~80 mg/L). Solution pH was adjusted to 3.0 ± 0.05 with dilute HCl, and crimp-sealed reactors were placed on an end-overend rotator and covered with aluminum foil. Reductive dissolution experiments at pH 5.5 were started by adding 10 mg of goethite solids to 120 mL of 10 mM ascorbic acid plus 5 mM acetic acid, and adjusting solution pH with dilute HCl or NaOH. At periodic intervals, aliquots were withdrawn from reactors, filtered through 0.2 μm nylon filters, and analyzed for aqueous Fe(II).

RESULTS AND DISCUSSION

Interpreting Enriched ^{57}Fe Isotope Tracer Experiments. We have previously used an enriched ^{57}Fe isotope tracer approach to demonstrate significant mixing of Fe between aqueous phase Fe(II) and bulk goethite with no formation of secondary minerals or change in size or shape of the particles.[28,48] Changes in the isotopic composition of either $Fe(II)_{aq}$ or goethite can be used to quantify the fractional approach of an isotope toward a completely mixed system. In isotope geochemistry, the standard approach for calculating the fractional approach toward complete mixing has been based on a linear relation as shown in eq 2.[57]

$$F = \text{Fractional approach toward complete mixing} = \frac{\delta_t - \delta_i}{\delta_{\mathrm{sys}} - \delta_i} \quad (2)$$

F refers to the fractional approach toward complete mixing of a specific isotope of Fe within the system, δ_t is the isotopic composition at time t, δ_i is the initial isotopic composition, and δ_{sys} is the isotopic composition for the entire system after complete mixing has occurred (in the absence of mass-dependent fractionations).

It is important to note, however, that although eq 2 may be useful for evaluating the extent of isotopic mixing, it does not describe the number of Fe atoms that have exchanged between Fe pools (e.g., $Fe(II)_{aq}$, goethite), particularly if the size of the Fe pools are different. For example, consider the case where we have a large pool of Fe in the mineral component and a small pool of Fe in the aqueous phase, as is the case for much of our previous work. For this case, the aqueous phase will need to "turnover" multiple times for the mineral phase to partially exchange, making the relative moles of Fe in each component an important variable to consider when determining percent of exchanged atoms in either component. The different amounts of Fe in each pool create a nonlinear relationship between changes in isotopic composition and extent of exchange that are not captured by eq 2.

To capture the nonlinearity created by different amounts of Fe in the aqueous and solid phase, we used a mass balance approach to derive equations for calculating the actual amount of Fe that has exchanged during reactions between $Fe(II)_{aq}$ and goethite (Gt) (see SI for derivation). Our approach is similar to Mikutta et al. (2009)[32] and results in the following when natural mass-dependent isotope fractionation is negligible:

$$\text{Percent Goethite Fe Exchange} = \frac{\mathrm{N}_{\mathrm{Fe(II)}} \times (\delta\mathrm{Fe(II)}^i_{aq} - \delta\mathrm{Fe(II)}^t)}{\mathrm{N}^{\mathrm{tot}}_{\mathrm{Gt}} \times (\delta\mathrm{Fe(II)}^t - \delta\mathrm{Gt}^i)} \times 100 \quad (3)$$

δ $Fe(II)^i_{aq}$ and δ Gt^i are the initial isotopic compositions of $Fe(II)_{aq}$ and goethite, respectively. $N_{Fe(II)}$ and N^{tot}_{Gt} are the moles of Fe(II) in the system and total moles of Fe in Gt. In low enrichment experiments it is important to include natural, mass-dependent isotope fractionation as it can become significant as the exchanging components approach the isotopic composition of the system:

$$\text{Percent Goethite Fe Exchange} = \frac{\mathrm{N}_{\mathrm{Fe(II)}} \times [\delta\mathrm{Fe(II)}^i_{\mathrm{aq}} - (\delta\mathrm{Fe(II)}^t - w_{\mathrm{Fe(II)}})]}{\mathrm{N}^{\mathrm{tot}}_{\mathrm{Gt}} \times [(\delta\mathrm{Fe(II)}^t - w_{\mathrm{Fe(II)}}) - \delta\mathrm{Gt}^i]} \times 100 \quad (4)$$

And

$$w_{\mathrm{Fe(II)}} = F \times \Delta \times \left(1 - \frac{\mathrm{N}_{\mathrm{Fe(II)}}}{\mathrm{N}^{\mathrm{tot}}_{\mathrm{Gt}} + \mathrm{N}_{\mathrm{Fe(II)}}}\right) \quad (5)$$

where Δ is the $Fe(II)_{aq}$-Gt equilibrium isotope fractionation factor in $\delta^{57/56}$Fe (‰); $\Delta^{57/56}\mathrm{Fe}_{\mathrm{Fe(II)aq\text{-}Gt}}$ for nano- and microgoethite is equal to −0.61 and −0.52 ‰, respectively.[47,54] A similar derivation is presented to estimate the percent goethite Fe exchanged based on changes in goethite isotopic compositions (eq 6 in SI).

Changes in the isotopic composition of $Fe(II)_{aq}$ enables accurate and consistent calculations of the fractional approach of the isotope tracer to complete mixing (eq 2), as well as the amount of Fe atom exchange (eqs 3 and 4). The difference between fractional approach to complete mixing (eq 2) and

percent of mineral exchange (eqs 3 and 4) can be significant especially at low Fe(II):Fe(III) ratios. For example, Figure 1

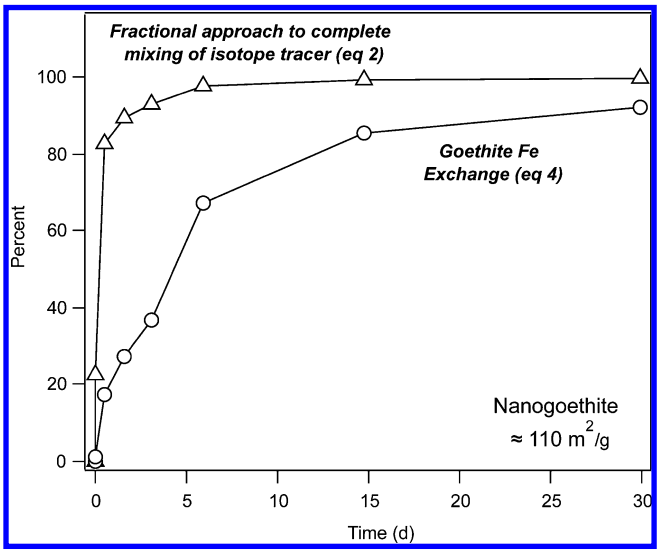

Figure 1. Comparison of models for interpreting ^{57}Fe(II)-enriched isotope tracer experiments with natural abundance goethite. The fractional approach to complete mixing of the ^{57}Fe enriched isotope tracer was calculated using eq 2 and the percent of goethite Fe exchange was calculated using eq 4. Reaction conditions: 1 mM initial aqueous Fe(II), 2 g L^{-1} nanogoethite, pH 7.5, 25 mM HEPES, and 25 mM KBr.

compares the fractional approach to complete mixing of the ^{57}Fe tracer as calculated by eq 2 with the percent of goethite Fe exchange as calculated by eq 4 for our previous work at pH 7.5 with nanogoethite particles (110 m^2/g).[28] When the isotopic composition of the enriched tracer attains a value close to the complete mixing isotopic composition (or remains close to the initial isotopic composition), the two approaches yield similar results. For the nanogoethite work, we observed that the isotopic composition of Fe(II)$_{aq}$ was nearly identical to the completely mixed isotopic composition of the system after 30 days and we reported near-complete (>95%) exchange of Fe atoms between the aqueous phase and goethite,[28] an estimate based on eq 2. This estimate, however, does not account for the different Fe pool sizes and does not provide a quantitative assessment of the number of Fe atoms that have exchanged in the aqueous phase or the goethite. In this case, since the isotopic composition of the enriched tracer was close to the completely mixed isotopic composition, recalculating the percent of Fe in goethite exchanged using eqs 3 and 4, rather than eq 2, does not significantly influence the original interpretation. Both eqs 3 and 4 still indicate that a significant proportion (~94% and 92% respectively) of the Fe(III) in goethite exchanges with Fe(II)$_{aq}$ (Figure 1). Note that Handler et al., 2009, and the present work, used a relatively high ^{57}Fe(II)$_{aq}$ enrichment of about 840 per mil (‰) so the effect of mass dependent isotope fractionation on the amount of exchange is quite small (~2% for the nanogoethite).

In contrast, reinterpretation of our previous enriched Fe isotope tracer results with magnetite and Al-substituted goethite results in more significant disparities.[33,37] In both of these cases, incomplete mixing of the isotope tracer had occurred and smaller Fe(II):Fe(III) ratios were used which leads to significant differences between the fractional approach to complete mixing (eq 2) and the percent of mineral atoms exchanged (eq 4). For the case of magnetite, eq 2 indicated that the enriched isotope tracer had moved ~54% toward complete mixing, but eq 4 indicates that only ~10% of stoichiometric magnetite underwent exchange (SI Figure S1). In our work with Al-substituted goethite, we observed that Fe exchange with the aqueous phase was less for Al-substituted goethite than for pure goethite. While this observation is still valid, the extent of exchange of the Al-substituted goethite is substantially less when we account for the significant differences in the amount of Fe in each pool and recalculate percent of mineral exchanged using eq 3 (i.e., eq 1 indicates ~10% mixing occurs in Al-substituted goethite, whereas eq 3 indicates that <1% exchange of the Al-substituted goethite occurs). Other studies have similarly reported the fractional approach toward complete mixing of enriched Fe tracers as percent exchange and, in cases where incomplete exchange has occurred, the true amounts of exchange are likely to be less than originally reported.[9,34−36,58−60] Note that interpreting fractional approach to complete mixing using eq 2 has not been limited to studies with Fe isotopes, but has been used for decades in a variety of other isotopic studies such as Mg, H, and O (e.g., refs 61−63). Although eq 2 is an accurate assessment of the degree to which an initial isotopic contrast is erased, we recommend against using it to estimate the number of atoms exchanged because it is potentially misleading depending upon specific experimental conditions.

Effect of Solution pH and Particle Size. To investigate the effect of pH and particle size on the extent of goethite exchanged, we conducted Fe isotope tracer experiments at pH 5.0 with both the microgoethite (590 × 42 nm; 40 ± 3 m^2/g) and nanogoethite (81 × 11 nm; 110 ± 7 m^2/g) and compared it with the pH 7.5 results, using otherwise similar experimental conditions (e.g., solids loading, aqueous Fe(II) concentration, etc.) other than the use of different buffers (HEPES vs acetate). pH 5.0 is well below the point of zero charge for goethite (pH_{zpc} ≈ 7.0 to 8.5[64]) and at this low pH, the goethite surface becomes net positively charged through the increased driving force for surface O atom protonation, leading to no detectable sorption of aqueous Fe(II) based on its measured concentration in solution (Figure 2). The isotope data, however, reveal that despite the lack of detectable sorption, there is some mixing of goethite Fe with aqueous Fe(II) as the $\delta^{57/56}$Fe of the aqueous Fe(II) decreases from 840.4‰ to 339.0‰ and the goethite increases from −0.1‰ to 20.0‰ over 30 days (Figure 2; SI Table S2 and S3). Figure 2 highlights how tracking changes in isotopic compositions can reveal dynamics that are not readily observed with concentration data.

While the changes in isotopic compositions for both aqueous Fe(II) and residual goethite at pH 5.0 were measurable, the changes were significantly less than we observed for pH 7.5 for both particle sizes (SI Table S2 and S3). Using the aqueous Fe(II) isotopic compositions and eq 3, as well as the goethite isotopic compositions and eq 6 in SI, we can calculate the percent of goethite Fe exchanged for both particle sizes at both pH values (SI Table S4). At pH 7.5 both nanogoethite (110 m^2/g) and microgoethite (40 m^2/g) exchanged a significant amount of Fe with the aqueous phase after 30 days (92 and 89%, respectively) (Figure 3). We found strong agreement between the percent goethite exchanged calculated from aqueous Fe(II) and goethite isotopic compositions (within 5%). At pH 5.0, the extent of exchange was significantly less with ≈7% of the Fe in the nanogoethite exchanging and only

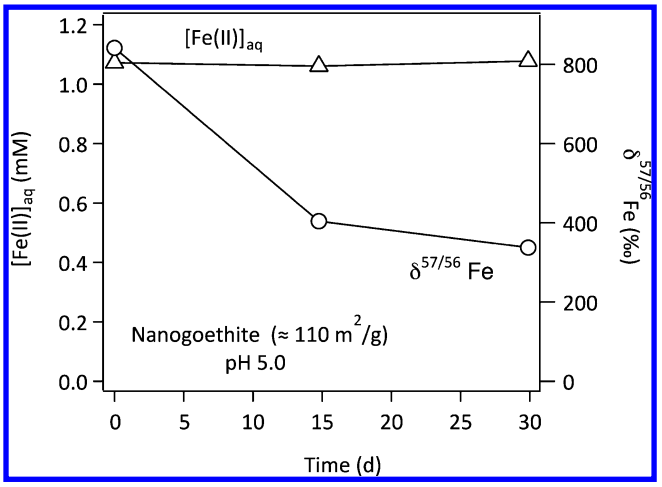

Figure 2. Comparison of aqueous Fe(II) concentrations and aqueous $\delta^{57/56}$Fe values for a ^{57}Fe(II)-enriched solution reacted with nanogoethite at pH 5.0. Reaction conditions: ∼ 1 mM initial aqueous Fe(II), initial $\delta^{57/56}$Fe = 840.43‰, 2 g L^{-1} nanogoethite, pH 5.0 NaAc buffer, and 25 mM KBr.

about 2% of Fe in the microgoethite exchanging (Figure 3). Using the specific surface area of each particle size, as well as available crystallographic information[65] to determine surface site density, we estimate that 20% of the Fe atoms are on the surface of the nanogoethite particles, whereas only about 7% of the Fe atoms are on the surface of the microgoethite particles (see SI for calculations). Therefore, at pH 7.5, significantly more than just surface Fe atoms are exchanging in contrast to pH 5.0 where the number of Fe atoms exchanged is less than the number of available surface Fe atoms.

The significant effect of pH on percent of goethite Fe atoms exchanging may partially explain the wide range of values reported in the literature. For example, Pedersen et al.[9] used goethite particles with a specific surface area similar to our microgoethite particles (37 compared to our 40 m^2/g) and at pH 6.6 observed about 15% of the goethite Fe exchanging after 16 days (estimated by applying eq 2). pH 6.6 is between the pH values of 5.0 and 7.5 used here and the % exchange also falls between the 7% and 92% we observed for nanogoethite at pH 5.0 and 7.5. Note, however, that pH is only one of several differences in the experimental conditions and it is likely that other experimental details, such as different synthesis methods (they used oxidation of $FeCO_3$ and we used hydrolysis) and a different Fe(II):Fe(III) mass ratio also play a role.

The most likely explanation for less exchange over 30 days at pH 5.0 compared to pH 7.5 is that little to no Fe(II) sorbs at pH 5.0 compared to almost half of the aqueous Fe(II) sorbing at pH 7.5 (Figure 2; SI Tables S2 and S3). With more Fe(II) sorbing to the goethite surface at pH 7.5, there is a higher probability of forming Fe(II)−goethite interfacial complexes that can lead to exchange of an Fe atom. While less Fe(II) sorption at pH 5.0 is the most obvious explanation for less goethite exchange at pH 5.0, changes in the energetics of electron transfer between aqueous Fe(II) and Fe(III) in goethite may also play a role. As the pH is lowered below the pH_{ZPC}, a higher surface charge develops which decreases the driving force for electron transfer.[66] It is also less likely that Fe(II) will sorb via an inner-sphere complex at the lower pH values because of the lower probability of deprotonated oxygen atoms that facilitate ligand exchange and bridge formation.[67] Formation of inner-sphere Fe(II) surface complexes has been shown to increase the electron transfer rate between Fe(II) donor and Fe(III) acceptor[68] and in the absence of forming an Fe(II) inner-sphere complex, electron transfer may be less favorable.

In addition, changes in aqueous Fe(II) speciation (due to different buffers) may have some influence on the extent of recrystallization observed at pH 5.0 and 7.5. Good's buffers, such as HEPES and MOPS, have been shown to affect redox reactions of Fe(II) with goethite.[69] Additional experiments are underway to explore the effect of Fe(II) aqueous speciation on extent of Fe(II)-catalyzed goethite recrystallization.

Interestingly, in addition to significantly less exchange observed at the lower pH value, there is also a difference in the effect of particle size on the percent of goethite exchanged. At pH 7.5, both particle sizes exchange similar amounts (92% and 89%, respectively) despite a 3-fold difference in surface area between nanogoethite and microgoethite (i.e., 110 and 40 m^2 g^{-1}, respectively). There is evidence, however, from some of our previous work that larger goethite particles exchange significantly less. Estimates of extent of Fe exchange for 20 and 13 m^2 g^{-1} goethite particles using eq 3 are as low as 3% and 1% after about 30 days, respectively.[37,47] Note, however, that these larger particles were both coarsened by heating (70 °C) in an

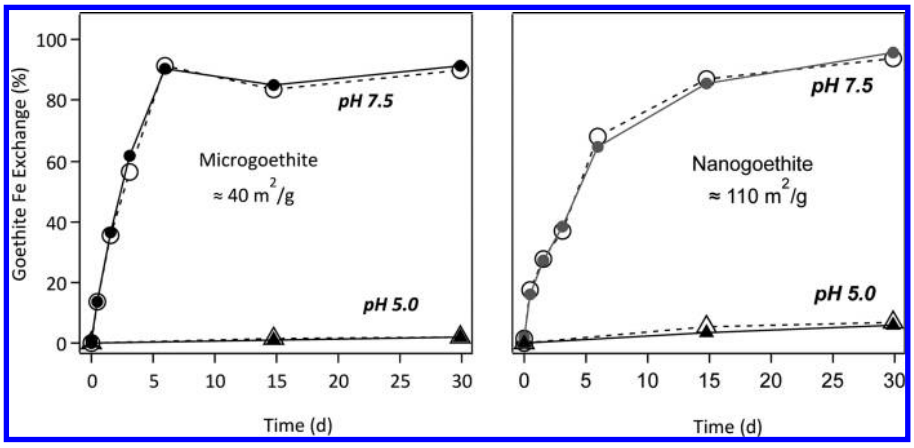

Figure 3. Effect of particle size and solution pH on percent of goethite exchanged in nanogoethite and microgoethite rods. Open markers were calculated from aqueous Fe(II) isotopic compositions using eq 4 and solid markers were calculated from goethite isotopic compositions using eq 6 in SI. Reaction conditions: 1 mM initial aqueous Fe(II), 2 g L^{-1} goethite, and 25 mM KBr (pH 7.5 was buffered with HEPES and pH 5.0 with NaAc).

alkaline fluid (pH ~ 13) for several days which may have influenced particle crystallinity as well as size, making it unclear if less exchange can be attributed to particle size alone.

In contrast, at pH 5.0 there is a distinct difference in the extent of exchange between the two particle sizes with markedly more exchange with the aqueous phase observed for the nanogoethite (7.0%) than the microgoethite (1.8%). One possible explanation for the different effect of particle size observed at pH 5.0 and 7.5 is a difference in aggregation behavior. We have previously shown that extensive aggregation of both the nanogoethite and microgoethite particles occurred at pH 7.5 resulting in particle aggregates of similar sizes.[48] The similar size of the particle aggregates may explain why we see no effect of particle size at pH 7.5 despite the significant difference in surface area. Indeed, we previously used aggregation to rationalize why we were observing similar Fe(II) sorption on both particle sizes despite an almost 3-fold difference in BET surface area.[48] As expected, at a much lower pH of 2.0, we observed little to no aggregation of the nanogoethite or microgoethite.[48] We speculate that at pH 5.0, which is well below the reported point of zero charge for goethite (pH 7.0 to 8.5[64]), there is less aggregation than at pH 7.5, and thus the exchange process has access to the true differences in particulate sizes and surface area. If true, this then means that surface-mediated steps, such as Fe(II) sorption or desorption may be rate-limiting for Fe(II)-catalyzed recrystallization of goethite, and that rates of exchange would then be controlled by the probability of Fe(II) interaction with the Fe oxide surface, which as discussed above is lower at pH 5.0 than at pH 7.5. This role of available surface area in determining extent of exchange at pH 5.0 is consistent with the roughly proportional increase in extent of exchange with increased surfaced area (a 3-fold increase in surface area results in an almost 4-fold increase in exchange).

We further developed a series of sequential extractions at each pH value for both particle sizes to gain additional insights into the exchange dynamics between goethite and aqueous Fe(II). The extractions were designed to separate the Fe(II)-goethite suspension into four operationally defined pools: aqueous Fe(II) (*centrifuged, filtered supernatant*), sorbed Fe(II) (*extract 1*), labile Fe(III) (*extracts 2 and 3*), and bulk goethite Fe(III) (*extract 4*) (SI Tables S2 and S3). At pH 7.5, *extract 1* recovered a majority of sorbed Fe(II) (>80%). No net Fe(II) sorption was observed at pH 5.0 and as expected *extract 1* recovered only trace levels of Fe. Despite using a lower HCl concentration to extract labile Fe(III) from the nanogoethite than microgoethite (1 M vs 1.75 M respectively), Fe(III) recoveries were higher for the nanogoethite. For both particle sizes, the amount of Fe(III) recovered in *extracts 2* and *3* is small accounting for less than 1% of the total Fe(III) in microgoethite and 3% of the total Fe(III) in the nanogoethite (less than a monolayer of Fe in both cases).

At pH 7.5, $\delta^{57/56}$Fe values in each of the extracts trend toward the completely mixed $\delta^{57/56}$Fe value of 37.6‰ and 37.8‰ for the nanogoethite and microgoethite, respectively over the course of 30 days (Figure 4; SI Tables S2 and S3). *Extract 1*, containing primarily sorbed Fe(II), had isotope ratios much lower than aqueous phase Fe(II) after 10 min of reaction. After a few hours, however, the $\delta^{57/56}$Fe values for aqueous Fe(II) and *extract 1* were quite similar and remained so for the duration of the experiment indicating that the aqueous Fe(II) and sorbed Fe(II) pools equilibrated within a few hours. *Extracts 2* and *3* became initially enriched in ^{57}Fe and rose above the completely mixed $\delta^{57/56}$Fe value before decreasing toward the completely mixed $\delta^{57/56}$Fe value. Accumulation of ^{57}Fe in the HCl extracted Fe(III) goethite components indicates that a gradient of ^{57}Fe develops within the goethite with more accumulation occurring in the more easily extracted Fe(III) (e.g., $\delta^{57/56}$Fe = 91‰ and 38‰ for *extract 2* and *extract 3* after 10 min). As exchange continued, however, $\delta^{57/56}$Fe values of *extract 2* approached those in *extract 3* (e.g., by 30 days, $\delta^{57/56}$Fe = 59‰ and 56‰ for *extract 2* and *extract 3*). Assuming a simplified conceptual model where the sequential extractions remove successively deeper layers of goethite, these results suggest that a ^{57}Fe gradient develops and there is a moving front progressing from the outer layers of the goethite toward the particle interior.

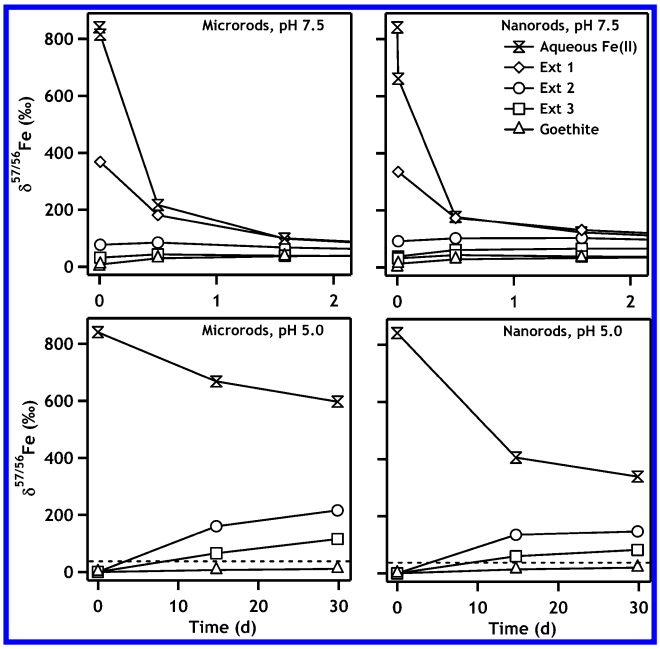

Figure 4. Measured $\delta^{57/56}$Fe values of sequential extractions performed on goethite solids after removal of aqueous Fe(II). Data collected at pH 7.5 is only displayed for the first 2 days to illustrate the initial gradient of ^{57}Fe that is observed in the experiment, showing a progression in $\delta^{57/56}$Fe of aqueous Fe(II) > *extract* 2 > *extract* 3 > residual goethite solids. Extract 1 contained primarily sorbed Fe(II), and therefore was not applicable in the pH 5.0 trials. Dashed lines indicate the delta value corresponding to complete mixing of the ^{57}Fe tracer, $\delta^{57/56}$Fe = 37.6 ‰.

At pH 5.0, *extracts 2* and *3* have a similar trend to pH 7.5 where both become enriched in ^{57}Fe with extract 2 initially more enriched than extract 3 (Figure 4). Unlike pH 7.5, however the two extracts do not begin to converge to similar values nor do they start decreasing to approach the completely mixed $\delta^{57/56}$Fe value. Interestingly the HCl extracted Fe(III) goethite components (*extracts 2* and *3*) appear to become more enriched at pH 5.0 then at pH 7.5. As noted above the percent of exchange that occurs at pH 5.0 is less than the available surface Fe atoms and perhaps the higher enrichments in the HCl extracted Fe(III) components reflects a smaller pool of Fe accessible for exchange (i.e., perhaps the bulk Fe is not available, via conduction, for exchange).

Particle Characterization before and After Fe(II)-Catalyzed Recrystallization. Despite ≈90% of the bulk Fe in the goethite particles exchanging with the aqueous phase at pH 7.5, we observed no changes in phase, crystallinity, particle

morphology or size of the goethite particles. We previously reported no change in size or phase for the nanogoethite particles, and present similar evidence here for the microgoethite with both XRD patterns and ^{57}Fe Mössbauer spectroscopy indicating the presence of only goethite after reaction of Fe(II) with the microgoethite (SI Figure S2 and S3). Particle size estimates from TEM images also reveal no noticeable change in size of the microgoethite before and after reaction with Fe(II) (SI Figure S4, Table S5). Note that based on initial HRTEM images of the nanogoethite, we previously speculated that reaction with aqueous Fe(II) may have made the nanogoethite more crystalline.[28] More extensive HRTEM imaging of nanogoethite particles performed in the current study, however, including imaging through rod widths (*a*- and *b*-axes) and along the long-axis of the rods (*c*-axis), revealed no detectable differences in crystallinity before or after reaction with aqueous Fe(II) (Figure 5). Furthermore, qualitative

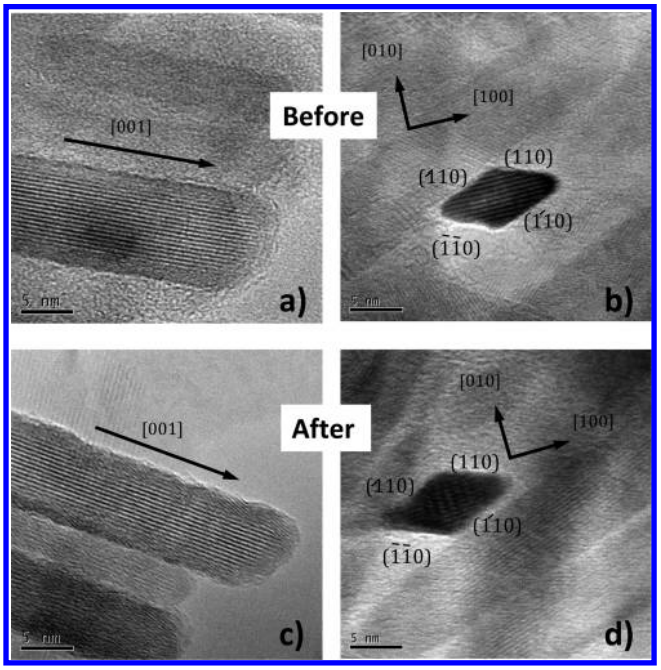

Figure 5. High-resolution cross-sectional TEM images of nanogoethite (110 m^2/g) before (a,b) and after (c,d) 30 day atom exchange reaction with Fe(II) at pH 7.5.

differences in crystal morphologies were not detected; the predominance of {110}[9,42] rod side faces (space group Pbnm) was similar in unreacted and Fe(II)-reacted goethite samples. No indication of preferential growth or dissolution at specific crystal faces was observed by HRTEM. Since there is no measurable change in particle size or morphology the process of recrystallization must involve spontaneous dissolution and reprecipitation processes, but in such a way that no measurable changes in the solid phase or bulk mineral lattice occurs other than Fe isotope exchange. This behavior seems inconsistent with traditional dissolution−reprecipitation mechanisms such as Ostwald ripening, where diffusive mass transport from small particles to large particles that are driven by surface free energy reduction can yield isotopic mixing without phase changes.[70] A mechanism, such as Ostwald ripening would be expected to result in progressive reduction in surface area of the solid, accompanied by shifting the particle size and possibly shape distribution, for which we see no evidence for in our experiments.

To determine whether the extensive recrystallization of goethite in the presence of Fe(II) impacted the macroscopic reactivity of the goethite particles, we measured rates of reductive dissolution by 10 mM ascorbic acid at pH 3.0 before and after reaction with aqueous Fe(II). At pH 3.0, we expected the particles to be stable and anticipated that little aggregation would occur based on our previous electron microscopy and dynamic light scattering studies of these particles, as conducted at pH 2.0.[48] As expected, nanogoethite dissolved faster than microgoethite (k_{obs} = 0.034 and 0.0126 d^{-1}, respectively) with the 2.7-fold increase in reduction rate most likely due to the 2.7-fold difference in specific surface areas (110 m^2/g and 40 m^2/g; resulting in surface area normalized rate coefficients of 3.1×10^{-4} and 3.2×10^{-4} g m^{-2} d^{-1}, respectively) between the two goethite particle sizes. Note that at the low pH of 3.0, aggregation is expected to be negligible as discussed above. Rates of reductive dissolution by ascorbic acid were nearly identical for goethite particles that had been mixed for 30 days in the presence or absence of Fe(II) suggesting that recrystallization does not influence the reactivity of the particles with regards to dissolution (at least reductive dissolution) (Figure 6). Similar rates of reductive dissolution is an

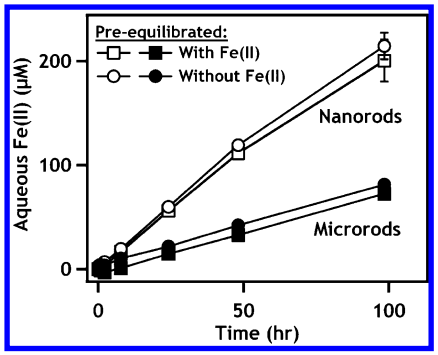

Figure 6. Reductive dissolution of nanogoethite (110 m^2/g) and microgoethite (40 m^2/g) at pH 3.0 using 10 mM ascorbic acid. Fe oxides were pre-equilibrated for 30 d in pH 7.5 buffer with (squares) or without (circles) 1 mM aqueous Fe(II), using conditions similar to ^{57}Fe isotope tracer studies. One-standard deviation based on triplicate batch reactors is contained within the margins of data markers in most instances.

observation that reinforces the conclusions of the HRTEM results indicating no changes in crystallinity despite 90% of the Fe atoms turning over due to exchange. What remains of key importance is to determine the mechanism responsible for such extensive recrystallization without measurable change in particle morphology, size, crystallinity, or reactivity.

While the present observations remain consistent with the bulk electron conduction mechanism invoked to explain atom exchange for the Fe(II)-goethite system in our previous study,[28] detailed aspects of the bulk electron conduction mechanism remain unaddressed. These include unresolved questions regarding (i) the operative distances of solid-state electrical current flow, and (ii) whether such current flows with a net preferred direction (e.g., predominantly from one crystal face or site-type to another) or are opposing and therefore mutually offsetting (i.e., no net current). The second question is particularly important because in the case of a net directional current, the source of an electrochemical potential gradient that

biases current flow should be identified. In the case of Fe(II)-hematite, chemically induced surface potential differences at structurally distinct crystal faces were identified as providing an electric gradient for net directional bulk conduction from relatively electronegative to electropositive faces.[43,71−73] Furthermore, a net directional current could also imply a free energy cost arising in the form of Joule heat dissipation in the solid due to electrical resistivity.[74,75] This aspect causes a dilemma for the single directional conveyor belt model we originally proposed, because it would require a thermodynamic driving force in the system that can be expended to overcome free energy lost to heat during sustained current flow through Fe oxide crystals. Additional experimental and theoretical work is underway to address these important, yet unresolved questions.

■ ASSOCIATED CONTENT

Supporting Information

Supporting Information is available and includes a derivation of the mass balance model, detailed calculations for estimating Fe atoms on the surface, particle characterization data, and tables including both chemical and isotopic data for exchange experiments. This material is available free of charge via the Internet at http://pubs.acs.org/.

■ AUTHOR INFORMATION

Corresponding Author

*Phone: 319-335-5654; fax: 319-335-5660; e-mail: michelle-scherer@uiowa.edu.

Present Address

[⊥]School of Civil Engineering and Geosciences, University of Newcastle upon Tyne, NE1 7RU, United Kingdom

Author Contributions

[#]Robert Handler and Andrew Frierdich contributed equally to this work.

Notes

The authors declare no competing financial interest.

■ ACKNOWLEDGMENTS

This work was supported by the National Science Foundation (NSF) through Grant No. EAR-1123978 and Award No. 1347848 and by the Geosciences Research Program at PNNL sponsored by the U.S. Department of Energy (DOE), Office of Basic Energy Sciences (BES), Division of Chemical Sciences, Geosciences & Biosciences. (BES provided support for K.R. and partial support for M.S.). A portion of this research was performed using EMSL, a national scientific user facility sponsored by the DOE's Office of Biological and Environmental Research and located at Pacific Northwest National Laboratory. Pacific Northwest National Laboratory (PNNL) is a multiprogram national laboratory operated for DOE by Battelle. We wish to thank Adrianna Heimann and Lingling Wu at UW-Madison for their assistance in sample preparation for mass spectrometry and Chris Gorski for his insightful comments on the paper.

■ REFERENCES

(1) Frederickson, J. K.; Zachara, J. M.; Kennedy, D. W.; Dong, H.; Onstott, T. C.; Hinmann, N. W.; Li, S.-M. Biogenic iron mineralization accompanying the dissimilatory reduction of hydrous ferric oxide by groundwater bacterium. *Geochim. Cosmochim. Acta.* **1998**, *62*, 3239−3257.

(2) Lovley, D. R.; Phillips, E. J. P. Novel mode of microbial energy-metabolism—Organic-carbon oxidation coupled to dissimilatory reduction of iron or manganese. *Appl. Environ. Microbiol.* **1988**, *54* (6), 1472−1480.

(3) Nealson, K. H.; Myers, C. R. Microbial reduction of manganese and iron: New approaches to carbon cycling. *Appl. Environ. Microbiol.* **1992**, *58* (2), 439−443.

(4) Schaetzl, R.; Anderson, S. *Soils: Genesis and Geomorphology*; Cambridge University Press: Cambridge, UK, 2005; p 817.

(5) Cutting, R. S.; Coker, V. S.; Fellowes, J. W.; Lloyd, J. R.; Vaughan, D. J. Mineralogical and morphological constraints on the reduction of Fe(III) minerals by *Geobacter sulfurreducens*. *Geochim. Cosmochim. Acta* **2009**, *73* (14), 4004−4022.

(6) Hansel, C. M.; Benner, S. G.; Fendorf, S. Competing Fe(II)-induced mineralization pathways of ferrihydrite. *Environ. Sci. Technol.* **2005**, *39*, 7147−7153.

(7) Hansel, C. M.; Benner, S. G.; Neiss, J.; Dohnalkova, A.; Kukkadapu, R.; Fendorf, S. Secondary mineralization pathways induced by dissmilatory iron reduction of ferrihydrate under advective flow. *Geochim. Cosmochim. Acta* **2003**, *67* (16), 2977−2992.

(8) Roden, E. E.; Urrutia, M. M. Influence of biogenic Fe(II) on bacterial crystalline Fe(III) oxide reduction. *Geomicrobiol. J.* **2002**, *19* (209), 209−251.

(9) Pedersen, H. D.; Postma, D.; Jakobsen, R.; Larsen, O. Fast transformation of iron oxyhydroxides by the catalytic action of aqueous Fe(II). *Geochim. Cosmochim. Acta* **2005**, *69* (16), 3967−3977.

(10) Borch, T.; Kretzschmar, R.; Kappler, A.; Cappellen, P. V.; Ginder-Vogel, M.; Voegelin, A.; Campbell, K. Biogeochemical redox processes and their impact on contaminant dynamics. *Environ. Sci. Technol.* **2009**, *44*, 15−23.

(11) Brown, G. E., Jr.; Parks, G. A. Sorption of trace elements on mineral surfaces: Modern perspectives from spectroscopic studies, and comments on sorption in the marine environment. *Int. Geol. Rev.* **2001**, *43*, 963−1073.

(12) Smedley, P. L.; Kinniburgh, D. G. A review of the source, behaviour and distribution of arsenic in natural waters. *Appl. Geochem.* **2002**, *17*, 517−568.

(13) Jickells, T. Atmospheric inputs of metals and nutrients to the oceans: Their magnitude and effects. *Mar. Chem.* **1995**, *48*, 199−214.

(14) Stumm, W.; Sulzberger, B. The cycling of iron in natural environments: Considerations based on laboratory studies of heterogeneous redox processes. *Geochim. Cosmochim. Acta* **1992**, *56* (8), 3233−3257.

(15) Neumann, A.; Hofstetter, T. B.; Skarpeli-Liati, M.; Schwarzenbach, R. P. Reduction of polychlorinated ethanes and carbon tetrachloride by structural Fe(II) in smectites. *Environ. Sci. Technol.* **2009**, *43* (11), 4082−4089.

(16) Fakih, M.; Davranche, M.; Dia, A.; Nowack, B.; Morin, G.; Petitjean, P.; Chatellier, X.; Gruau, G. Environmental impact of As(V)-Fe oxyhydroxide reductive dissolution: An experimental insight. *Chem. Geol.* **2009**, *259* (3−4), 290−303.

(17) Gregory, K. B.; Larese-Casanova, P.; Parkin, G. F.; Scherer, M. M. Abiotic transformation of hexahydro-1,3,5-trinitro-1,3,5-triazine by Fe^{II} bound to magnetite. *Environ. Sci. Technol.* **2004**, *38* (5), 1408−1414.

(18) Hofstetter, T. B.; Heijman, C. G.; Haderlein, S. B.; Schwarzenbach, R. P. In *Abiotic Reduction of Nitroaromatic Explosives under Sulfate- And Iron-Reducing Conditions*, 213th National Meeting, San Francisco, CA, 1997; Division of Environmental Chemistry, American Chemical Society, 1997; pp 118−119.

(19) Kenneke, J. F.; Weber, E. J. Reductive dehalogenation of halomethanes in iron- and sulfate-reducing sediments. 1. Reactivity pattern analysis. *Environ. Sci. Technol.* **2003**, *37* (4), 713−720.

(20) Tai, Y. L.; Dempsey, B. A. Nitrite reduction with hydrous ferric oxide and Fe(II): Stoichiometry, rate, and mechanism. *Water Res.* **2009**, *43* (2), 546−552.

(21) Elsner, M.; Schwarzenbach, R. P.; Haderlein, S. B. Reactivity of Fe(II)-bearing minerals toward reductive transformation of organic contaminants. *Environ. Sci. Technol.* **2004**, *38* (3), 799−807.

(22) Jang, J. H.; Dempsey, B. A.; Catchen, G. L.; Burgos, W. D. Effects of Zn(II), Cu(II), Mn(II), Fe(II), NO_3^-, or SO_4^{2-} at pH 6.5 and 8.5 on transformations of hydrous ferric oxide (HFO) as evidenced by Mossbauer spectroscopy. *Colloid. Surf. A* **2003**, *221* (1−3), 55−68.
(23) Peretyazhko, T.; Zachara, J. M.; Heald, S. M.; Jeon, B. H.; Kukkadapu, R. K.; Liu, C.; Moore, D.; Resch, C. T. Heterogeneous reduction of Tc(VII) by Fe(II) at the solid-water interface. *Geochim. Cosmochim. Acta* **2008**, *72* (6), 1521−1539.
(24) Boyanov, M. I.; O'Loughlin, E. J.; Roden, E. E.; Fein, J. B.; Kemner, K. M. Adsorption of Fe(II) and U(VI) to carboxyl-functionalized microspheres: The influence of speciation on uranyl reduction studied by titration and XAFS. *Geochim. Cosmochim. Acta* **2007**, *71* (8), 1898−1912.
(25) Jeon, B.-H.; Dempsey, B. A.; Burgos, W. D.; Barnett, M. O.; Roden, E. E. Chemical reduction of U(VI) by Fe(II) at the solid-water interface using natural and synthetic Fe(III) oxides. *Environ. Sci. Technol.* **2005**, *39* (15), 5642−5649.
(26) Yang, L.; Steefel, C. I.; Marcus, M. A.; Bargar, J. R. Kinetics of Fe(II)-catalyzed transformation of 6-line ferrihydrite under anaerobic flow conditions. *Environ. Sci. Technol.* **2010**, *44* (14), 5469−5475.
(27) Tamaura, Y.; Ito, K.; Katsura, T. Transformation of γ-FeO(OH) to Fe_3O_4 by adsorption of iron(II) ion on γ-FeO(OH). *Chem. Soc. Dalton Trans.* **1983**, 189−194.
(28) Handler, R. M.; Beard, B. L.; Johnson, C. M.; Scherer, M. M. Atom exchange between aqueous Fe(II) and goethite: An Fe isotope tracer study. *Environ. Sci. Technol.* **2009**, *43*, 1102−1107.
(29) Crosby, H. A.; Johnson, C. M.; Roden, E. E.; Beard, B. L. Coupled Fe(II) -Fe(III) electron and atom exchange as a mechanism for Fe isotope fractionation during dissimilatory iron oxide reduction. *Environ. Sci. Technol.* **2005**, *39* (17), 6698−6704.
(30) Crosby, H. A.; Roden, E. E.; Johnson, C. M.; Beard, B. L. The mechanisms of iron isotope fractionation produced during dissimilatory Fe(III) reduction by *Shewanella putrefaciens* and *Geobacter sulfurreducens*. *Geobiology* **2007**, *5* (2), 169−189.
(31) Jang, J. H.; Mathur, R.; Liermann, L. J.; Ruebush, S.; Brantley, S. L. An iron isotope signature related to electron transfer between aqueous ferrous iron and goethite. *Chem. Geol.* **2008**, *250* (1−4), 40−48.
(32) Mikutta, C.; Wiederhold, J. G.; Cirpka, O. A.; Hofstetter, T. B.; Bourdon, B.; Gunten, U. V. Iron isotope fractionation and atom exchange during sorption of ferrous iron to mineral surfaces. *Geochim. Cosmochim. Acta* **2009**, *73*, 1795−1812.
(33) Gorski, C. A.; Handler, R. M.; Beard, B. L.; Pasakarnis, T.; Johnson, C. M.; Scherer, M. M. Fe Atom exchange between aqueous Fe^{2+} and magnetite. *Environ. Sci. Technol.* **2012**, *46*, 12399−12407.
(34) Jones, A. M.; Collins, R. N.; Rose, J.; Waite, T. D. The effect of silica and natural organic matter on the Fe(II) -catalysed transformation and reactivity of Fe(III) minerals. *Geochim. Cosmochim. Acta* **2009**, *73* (15), 4409−4422.
(35) Wu, L.; Beard, B. L.; Roden, E. E.; Johnson, C. M. Stable iron isotope fractionation between aqueous Fe(II) and hydrous ferric oxide. *Environ. Sci. Technol.* **2011**, *45*, 1847−1852.
(36) Frierdich, A. J.; Scherer, M. M.; Bachman, J. E.; Engelhard, M. H.; Rapponotti, B. W.; Catalano, J. G. Inhibition of trace element release during Fe(II) -activated recrystallization of Al-, Cr-, and Sn-substituted goethite and hematite. *Environ. Sci. Technol.* **2012**, *46*, 10031−10039.
(37) Latta, D. E.; Bachman, J. E.; Scherer, M. M. Fe electron transfer and atom exchange in goethite: Influence of Al-substitution and anion sorption. *Environ. Sci. Technol.* **2012**, *46*, 10614−10623.
(38) Masue-Slowey, Y.; Loeppert, R. H.; Fendorf, S. Alteration of ferrihydrite reductive dissolution and transformation by adsorbed As and structural Al: Implications for As retention. *Geochim. Cosmochim. Acta* **2011**, *75* (3), 870−886.
(39) Frierdich, A. J.; Catalano, J. G. Fe(II) -mediated reduction and repartitioning of structurally incorporated Cu, Co, and Mn in iron oxides. *Environ. Sci. Technol.* **2012**, *46*, 11070−11077.
(40) Frierdich, A. J.; Catalano, J. G. Controls on Fe(II) -activated trace element release from goethite and hematite. *Environ. Sci. Technol.* **2012**, *46*, 1519−1526.
(41) Frierdich, A. J.; Luo, Y.; Catalano, J. G. Trace element cycling through iron oxide minerals during redox driven dynamic recrystallization. *Geology* **2011**, *39*, 1083−1086.
(42) Latta, D. E.; Gorski, C. A.; Scherer, M. M. Influence of Fe^{2+}-catalysed iron oxide recrystallization on metal cycling. *Biochem. Soc. Trans.* **2012**, *40*, 1191−1197.
(43) Yanina, S. V.; Rosso, K. M. Linked reactivity at mineral-water interfaces through bulk crystal conduction. *Science* **2008**, *320*, 218−222.
(44) Gorski, C. A.; Scherer, M. M., Fe^2+ sorption at the fe oxide-water interface: A revised conceptual framework. In *Aquatic Redox Chemistry*; Tratnyek, P. G., Grundl, T. J., Haderlein, S. B., Eds.; Oxford University Press: Washington DC, 2011.
(45) Wu, L.; Beard, B. L.; Roden, E. E.; Johnson, C. M. Influence of pH and dissolved Si on Fe isotope fractionation during dissimilatory microbial reduction of hematite. *Geochim. Cosmochim. Acta* **2009**, *73*, 5584−5599.
(46) Wu, L.; Beard, B. L.; Roden, E. E.; Kennedy, C. B.; Johnson, C. M. Stable Fe isotope fractionations produced by aqueous Fe(II)—Hematite surface interactions. *Geochim. Cosmochim. Acta* **2010**, *74*, 4249−4265.
(47) Frierdich, A. J.; Beard, B. L.; Reddy, T. R.; Scherer, M. M.; Johnson, C. M. Iron isotopic fractionation between aqueous Fe(II) and goethite revisited: New insights based on a multi-direction approach to equilibrium and isotopic exchange rate modification. *Geochim. Cosmochim. Acta* **2014**, *139*, 383−398.
(48) Cwiertny, D. M.; Handler, R. M.; Schaefer, M. V.; Grassian, V. H.; Scherer, M. M. Interpreting nanoscale size-effects in aggregated Fe-oxide suspensions: Reaction of Fe(II) with goethite. *Geochim. Cosmochim. Acta* **2008**, *72* (5), 1365−1380.
(49) Burleson, D. J.; Penn, R. L. Two-step growth of goethite from ferrihydrite. *Langmuir* **2006**, *22* (1), 402−409.
(50) Schwertmann, U.; Cornell, R. M. *Iron Oxides in the Laboratory: Preparation and Characterization*, 2nd ed.; Wiley-VCH: Weinheim, 2000; p 188.
(51) Fortune, W. B.; Mellon, M. G. Determination of iron with o-phenanthroline—A spectrophotometric study. *Ind. Eng. Chem. Anal. Ed.* **1938**, *10*, 0060−0064.
(52) Tamura, H.; Goto, K.; Yotsuyan, T.; Nagayama, M. Spectrophotometric determination of iron(II) with 1,10-phenanthroline in presence of large amounts of iron(III). *Talanta* **1974**, *21* (4), 314−318.
(53) Beard, B. L.; Johnson, C. M.; Skulan, J. L.; Nealson, K. H.; Cox, L.; Sun, H. Application of Fe isotopes to tracing the geochemical and biological cycling of Fe. *Chem. Geol.* **2003**, *195* (1−4), 87−117.
(54) Beard, B. L.; Handler, R. M.; Scherer, M. M.; Wu, L.; Czaja, A. D.; Heimann, A.; Johnson, C. M. Iron isotope fractionation between aqueous ferrous iron and goethite. *Earth Planet. Sc. Lett.* **2010**, *295*, 241−250.
(55) Beard, B. L.; Johnson, C. M. High precision iron isotope measurements of terrestrial and lunar materials. *Geochim. Cosmochim. Acta* **1999**, *63* (11−12), 1653−1660.
(56) Postma, D. The reactivity of iron oxides in sediments: A kinetic approach. *Geochim. Cosmochim. Acta* **1993**, *57* (21−22), 5027−5034.
(57) Criss, R. E. *Principles of Stable Isotope Distribution*; Oxford University Press: New York, 1999.
(58) Guilbaud, R.; Butler, I. B.; Ellam, R. M.; Rickard, D. Fe isotope exchange between $Fe(II)_{aq}$ and nanoparticulate mackinawite (FeS_m) during nanoparticle growth. *Earth Planet. Sci. Lett.* **2010**, *300*, 174−183.
(59) Guilbaud, R.; Butler, I. B.; Ellam, R. M.; Rickard, D.; Oldroyd, A. Experimental determination of the equilibrium Fe isotope fractionation between Fe^{2+} and FeS_m (mackinawite) at 25 and 2°C. *Geochim. Cosmochim. Acta* **2011**, *75*, 2721−2734.
(60) Wu, L.; Percak-Dennett, E. M.; Beard, B. L.; Roden, E. E.; Johnson, C. M. Stable iron isotope fractionation between aqueous

Fe(II) and model Archean ocean Fe−Si coprecipitates and implications for iron isotope variations in the ancient rock record. *Geochim. Cosmochim. Acta* **2012**, *84*, 14−28.
(61) Graham, C. M. Experimental hydrogen isotope studies III: Diffusion of hydrogen in hydrous minerals, and stable isotope exchange in metamorphic rocks. *Contrib. Mineral. Petrol.* **1981**, *76*, 216−228.
(62) Li, W.; Beard, B. L.; Johnson, C. M. Exchange and fractionation of Mg isotopes between epsomite and saturated $MgSO_4$ solution. *Geochim. Cosmochim. Acta* **2011**, *75*, 1814−1828.
(63) Northrop, D. A.; Clayton, R. N. Oxygen-isotope fractionations in systems containing dolomite. *J. Geol.* **1966**, 174−196.
(64) Kosmulski, M. *Chemical Properties of Material Surfaces*; CRC Press: New York, 2001.
(65) Gualtieri, A. F.; Venturelli, P. In situ study of the goethite-hematite phase transformation by real time synchrotron powder diffraction. *Am. Mineral.* **1999**, *84* (5−6), 895−904.
(66) Hiemstra, T.; van Riemsdijk, W. H. Adsorption and surface oxidation of Fe(II) on metal (hydr) oxides. *Geochim Cosmochim Acta* **2007**, *71* (24), 5913−5933.
(67) Casey, W. H. A view of reactions at mineral surfaces from the aqueous phase. *Mineral. Mag.* **2001**, *65* (3), 323−337.
(68) Kerisit, S.; Rosso, K. M., Charge transfer in FeO: A combined molecular-dynamics and ab initio study. *J. Chem. Phys.* **2005**, *123*, (22).
(69) Buchholz, A.; Laskov, C.; Haderlein, S. B. Effects of zwitterionic buffers on sorption of ferrous iron at goethite and its oxidation by CCl_4. *Environ. Sci. Technol.* **2011**, *45* (8), 3355−3360.
(70) Stoffregen, R. Numerical simulation of mineral-water isotope exchange via Ostwald ripening. *Am. J. Sci.* **1996**, *296* (8), 908−931.
(71) Boily, J. F.; Chatman, S.; Rosso, K. M. Inner-Helmholtz potential development at the hematite (alpha-Fe_2O_3) (001) surface. *Geochim. Cosmochim. Acta* **2011**, *75* (15), 4113−4124.
(72) Chatman, S.; Zarzycki, P.; Preoanin, T.; Rosso, K. M. Effect of surface site interactions on potentiometric titration of hematite (alpha-Fe_2O_3) crystal faces. *J. Colloid Interface Sci.* **2013**, *391*, 125−134.
(73) Chatman, S.; Zarzycki, P.; Rosso, K. M. Surface potentials of (001), (012), (113) hematite (alpha-Fe_2O_3) crystal faces in aqueous solution. *Phys. Chem. Chem. Phys.* **2013**, *15* (33), 13911−13921.
(74) Zarzycki, P.; Smith, D. M. A.; Rosso, K. M. Proton dynamics on goethite nanoparticles and coupling to electron transport. *J. Chem. Theory Comput.*, in review.
(75) Rohsenow, W.; Hartnett, J.; Ganic, E. *Handbook of Heat Transfer Fundamentals*; McGraw-Hill Book Co.: New York, NY, 1985; Vol. *1*.